

Fabrication of Various Ordered Films of Oxotitanium(IV) Phthalocyanine by Vacuum Deposition and Their Spectroscopic Behavior

Hisatomo Yonehara,[†] Hideki Etori,[†] M. K. Engel,[†] Minoru Tsushima,[‡]
Noriaki Ikeda,[‡] Takeshi Ohno,[‡] and Chyongjin Pac^{*,†}

Kawamura Institute of Chemical Research, 631 Sakado, Sakura, Chiba 285-0078, Japan, and
Department of Chemistry, Graduate School of Science, Osaka University, 1-16 Toyonaka,
Osaka 560-0043, Japan

Received September 22, 2000. Revised Manuscript Received December 6, 2000

Different types of ordered solid films of oxotitanium(IV) phthalocyanine (OTiPc) were grown in 50–500 nm thickness by vacuum deposition onto such conventional substrates as metal- and ITO-coated glass and neat glass at a rate of $\sim 0.05 \text{ nm s}^{-1}$. Under 10^{-3} – 10^{-4} Pa isotropic films with short-range molecular organization and preferential molecular orientation were grown on the substrates kept at ~ 25 °C but ordered α (phase II) or β (phase I) crystal films on the substrates heated at 150 °C. The deposition onto surface-oxidized Al, Ti, and Cu/glass, ITO/glass, and neat glass at ~ 25 or 150 °C selectively gave ordered isotropic or α -crystal films which have preferential molecular alignments with “standing” orientations of the molecular plane with respect to the substrate surface. On the other hand, another type of ordered isotropic or β -crystal films with preferential “lying” molecular orientations was formed by the deposition onto Au, Ag, and unoxidized Cu on glass at ~ 25 or 150 °C. In the case of 150 °C-heated Pt/glass, the α -crystal film with “standing” molecular orientations was grown under 10^{-3} – 10^{-4} Pa, but another type of α -crystal film with “lying” orientations under 2.7×10^{-5} Pa. Scanning electron microscopic observations of the ordered crystalline films indicated that single-crystal-like domains are grown from the bottom to the top of the film and are densely packed to give monolithic morphologies with little grain boundary. Visible–near-IR absorption and fluorescence spectra of the ordered solid films were recorded, showing unique dependences on the molecular alignments involving anisotropic behavior in the polarized absorption spectra of the α -crystal films with different molecular alignments.

Phthalocyanines (MPc's), a typical family of fully π -conjugated macrocyclic molecules with remarkable chemical stabilities and versatile functionalities, are known not only as “classical dyes” in practical use but also as “modern functional materials” in scientific researches as well as in applications to organic electronic devices.^{1–4} In general, the planar MPc macrocycles can stack in a variety of modes to give polymorphic crystals,^{5,6} which reveal very often different solid-state electronics and functionalities depending upon the crystal structures (i.e., molecular alignments).^{2,3} Oxotitanium(IV) phthalocyanine (OTiPc) is of interest associated with the solid-state photofunctionalities, because this particular OTiPc crystalline material is known as one of the most sensitive organic photo-

conductors used in electrophotographic devices.^{2–4} This molecule has a shallow square-pyramid structure (Figure 1) which may be related with formation of characteristic polymorphic crystals.^{6,7}

Although strong dependences of photoconductivity on the crystalline phases of MPc's have been reported,^{2–4,8} most studies on the photoconductive functions of MPc's have been carried out, from practical viewpoints, for polymer-dispersed films of microcrystalline particles, in which microcrystals are randomly oriented. The solid-state electronics of MPc associated with the molecular alignments in particular crystalline phases should be anisotropic, and hence the understanding of the anisotropic nature certainly requires suitable materials that must be not only ordered in molecular alignment but also relevant in size for various measurements of the electronic properties. Extensive efforts have been made on fabrication of highly ordered assemblies of MPc's by modified Langmuir–Blodgett (LB) methods^{9,10} as well as by molecular-beam epitaxy (MBE) and molecular-

[†] Kawamura Institute of Chemical Research.

[‡] Osaka University.

(1) Simon, J.; Andre, J.-J. In *Molecular Semiconductors*; Springer-Verlag: Berlin, 1985.

(2) Bosenberger, P. M.; Weiss, D. S. In *Organic Photoreceptors for Imaging Systems*; Marcel Dekker: New York, 1993.

(3) Law, K. Y. *Chem. Rev.* **1993**, *93*, 449.

(4) Fujimaki, Y.; Tadokoro, H.; Oda, Y.; Yoshioka, H.; Homma, T.; Moriguchi, H.; Watanabe, K.; Konishita, A.; Hirose, N.; Itami, A.; Ikeuchi, S. *J. Imaging Technol.* **1991**, *17*, 202.

(5) Mark, W. T. C.; Zhou, G. D. In *Crystallography in Modern Chemistry*; J. Wiley: New York, 1992; pp 578–588.

(6) Hiller, W.; Strähle, J.; Kobel, W.; Hanack, M. *Z. Kristallografia* **1982**, *159*, 173.

(7) Jennings, C. A.; Aroca, R.; Kovacs, G. J.; Hsiao, C. *J. Raman Spectrosc.* **1996**, *27*, 867.

(8) Enokida, T.; Hirohashi, R.; Nakamura, T. *J. Imaging Sci.* **1990**, *34*, 234.

(9) (a) Ogawa, K.; Yonehara, H.; Pac, C. *Langmuir* **1994**, *10*, 2068.
(b) Ogawa, K.; Yonehara, H.; Pac, C. *Mol. Cryst. Liq. Cryst.* **1995**, *258*, 315.

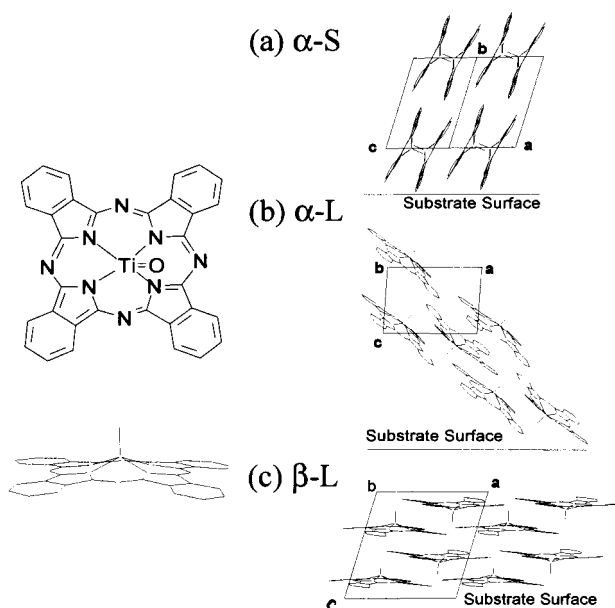


Figure 1. Molecular structure of oxotitanium(IV) phthalocyanine (OTiPc) and molecular orientation models for (a) α -S, (b) α -L, and (c) β -L. For the abbreviations, see text.

beam deposition (MBD) under ultrahigh vacuum (UHV, $<10^{-5}$ Pa) using particular substrates.^{11–20} However, these elegant methods have serious difficulties in fabricating “tough and thick” solid films with a series of different molecular alignments on conventional substrates. This seems to limit applications of these methods to the construction of practical electronic devices, e.g., sandwich-type cells.

On the other hand, conventional vacuum deposition is certainly an effective way to obtain such tough and thick solid films but has been thought to be difficult in controlling molecular alignments. In a previous paper,²¹ we reported that conventional vacuum deposition of OTiPc onto a glass substrate at a low deposition rate gives ordered films, which we call “amorphous-like” films with preferential molecular orientation since the visible absorption spectra are characteristic of amorphous OTiPc. Notably, highly ordered solid films of CuPc and OTiPc are grown on such conventional substrates as amorphous quartz¹⁹ and sapphire²⁰ though an MBD technique was used under UHV. These find-

ings encouraged us to investigate detailed conditions for conventional vapor deposition of OTiPc onto various conventional substrates, under which molecular alignments in the deposited films can be controlled. In this paper, we wish to report our successful attempts for the fabrication of a series of ordered solid films of OTiPc by vapor deposition onto conventional substrates.

Experimental Section

Visible–near-infrared (VNIR) transmission–absorption spectra were obtained on an Otsuka MCPD-1000 spectrometer. A Bio-Rad FTS-60A spectrometer was used for IR transmission–absorption and reflection–absorption spectra (RAS); a Spectra-Mono attachment combined with a polarizer was used for the latter. X-ray diffraction (XRD) was recorded on a Rigaku Ru-200B X-ray diffractometer equipped with a thin-film attachment using CuK monochromatic radiation at an angle of 2° made by the incident beam with the sample surface. The film thickness was determined with a Sloan Dektak 3030ST surface profiler. A Hitachi S-800 instrument was used for scanning electron microscopic (SEM) observations under typical acceleration voltage of 10 KV after platinum coating (2 nm). Fluorescence spectra were taken for the emissions from the front side (surface) of films excited at an incident angle of 30° using a Coherent Innova 306 Ar laser (514.5 nm, 50 mW) or an NEC GLG5010 He–Ne laser (632.8 nm, 5 mW) as the excitation light source and a Jasco CT-250 grating monochromator with a silicon diode array detector (Hamamatsu S3901–512Q).

Semitransparent metal-on-glass substrates were obtained by evaporating Cu, Ag, Au, Ti, and Al on 1 mm thick Corning 7059 glass plates (20×20 mm²) at 0.2 nm s⁻¹ under 1×10^{-3} – 10^{-5} Pa and by sputtering Pt onto the glass plate at 0.1 nm s⁻¹; the thickness of the metal films was ca. 20 nm. Indium–tin-oxide (ITO) substrates (40 nm thick ITO layer on Corning 7059 glass) were purchased from GEOMATEC Co., and Corning 7059 glass plates were also used as substrate. The OTiPc compound free from H₂Pc and other observable impurities was obtained by repeated vacuum sublimation of a sample prepared according to a known method.²² Deposition was performed by heating OTiPc powders in an alumina crucible ($10^6 \times 10^4$ mm) at 380 – 420 °C under 1×10^{-3} – 1×10^{-4} Pa or in a Knudsen cell ($10^6 \times 100^4$ mm) at 230 – 260 °C under 2.7×10^{-5} Pa while the substrates were kept at ambient temperature (~ 25 °C) or at a temperature of 100 – 250 °C. For experimental convenience, in most cases, the vacuum of the chamber was broken after the metal coating, and then the OTiPc source was introduced into the chamber for the deposition. As comparable runs, in situ deposition was performed under keeping the vacuum after the metal coating on glass. The deposition rate was monitored with a quartz-crystal thickness monitor after correction with the film thickness determined by the surface profiler. The substrates were set upward at 20 cm from the top of the OTiPc source to prevent thermal effects from the heater. For the organic-vapor-induced phase change of a-S and a-L, the films were placed in a desiccator where a flask filled with liquid CH₂Cl₂ had been set and then stored for greater than 12 h at room temperature.

Results and Discussion

Deposition onto Various Substrates Kept at Ambient Temperature. In preliminary experiments where the deposition rates were changed from 0.01 to 1.5 nm s⁻¹, it was confirmed that a deposition rate at ~ 0.05 nm s⁻¹ is practically suitable for the fabrication of ordered films while random molecular orientations occurred by deposition at ≥ 0.1 nm s⁻¹.²¹ In this work,

(10) Ogawa, K.; Yao, J.; Yonehara, H.; Pac, C. *J. Mater. Chem.* **1996**, *6*, 143.

(11) Forrest, S. R. *Chem. Rev.* **1997**, *97*, 1793.

(12) Saito, E.; Uyeda, N.; Ashida, M. *Nature* **1962**, *194*, 273.

(13) Hara, M.; Sasabe, H.; Yamada, A.; Garito, A. F. *Jpn. J. Appl. Phys.* **1989**, *28*, L306.

(14) Dann, A. J.; Hoshi, H.; Maruyama, Y. *J. Appl. Phys.* **1990**, *67*, 1371.

(15) Chau, L.-K.; Arbour, C.; Collins, G. E.; Nebesny, K. W.; Lee, P. A.; England, C. D.; Armstrong, N. R.; Parkinson, B. A. *J. Phys. Chem.* **1993**, *97*, 2690.

(16) Chau, L.-K.; England, C. D.; Chen, S.; Armstrong, N. R. *J. Phys. Chem.* **1993**, *97*, 2699.

(17) Schmidt, A.; Chau, L.-K.; Back, A.; Armstrong, N. R. In *Phthalocyanines: Properties and Applications*; Leznoff, C. C., Lever, A. B. P., Eds.; VCH Publishers: New York, 1996; Vol. 4, pp 307–341.

(18) Tokito, S.; Sakata, J.; Taga, Y. *Thin Solid Films* **1995**, *256*, 182.

(19) Komiyama, M.; Sakakibara, Y.; Hirai, H. *Thin Solid Films* **1987**, *151*, L109.

(20) Yamashita, A.; Maruno, T.; Hayashi, T. *J. Phys. Chem.* **1994**, *98*, 12695.

(21) Yonehara, H.; Pac, C. *Mater. Res. Soc. Symp. Proc.* **1994**, *328*, 301.

(22) Yao, J.; Yonehara, H.; Pac, C. *Bull. Chem. Soc. Jpn.* **1995**, *68*, 1001.

Table 1. Ordered Solid Films of OTiPc Deposited onto Various Substrates

deposition conditions ^b	solid films ^a				
	a-S	a-L	α -S	α -L	β -L
substrates ^c	Pt Al, Ti, Cu ^d , ITO, glass	Au, Ag	Pt Al, Ti, Cu ^d , ITO, glass	Pt	Au, Ag, Cu ^e
substrate temp. (°C)	~25	~25	150	150	150
pressure (Pa)	10^{-3} – 10^{-4}	10^{-3} – 10^{-4}	10^{-3} – 10^{-4}	2.7×10^{-5}	10^{-3} – 10^{-4}

^a Key: a = amorphous-like, α = α (phase II) crystal, β = β (phase I) crystal, S = standing molecular orientation, and L = lying molecular orientation; see text. ^b At a deposition rate of 0.05 nm s⁻¹. ^c Metal-coated or indium–tin oxide (ITO)-coated glass substrates and neat glass plates. ^d Air-exposed Cu/glass substrate. ^e In situ deposition onto a Cu/glass substrate unexposed to air; see text.

therefore, the deposition was performed at a rate of ~ 0.05 nm s⁻¹ under various conditions. Table 1 summarizes the major results. For convenience, the films fabricated are abbreviated as a-S, a-L, α -S, α -L, and β -L where the notation “a”, “ α ”, or “ β ” denotes the amorphous-like, α -crystal (phase II), or β -crystal (phase I) form each, and the letters “S” and “L” mean “standing” and “lying” molecular orientations, respectively (Figure 1).

The solid films of OTiPc deposited onto Pt, Cu, Al, and ITO on glass and onto neat glass at ambient temperature (~ 25 °C) under 1×10^{-3} – 2.7×10^{-5} Pa showed common VNIR spectra ($\lambda_{\max} = 720$, ~ 650 (sh) nm) as well as common XRD patterns (a peak at $2\theta = 6.85^\circ$ ($d = 1.29$ nm) and the broad halo from the substrate at $2\theta > 15^\circ$) (Figure 2a,c). Since the VNIR spectra are characteristic of amorphous OTiPc,^{8,21} we call these films, for convenience, amorphous-like films denoted as a-S. The appearance of the single XRD peak indicates that a-S is more or less ordered in molecular alignment. The ordered character of a-S was further indicated by a systematic change of the *p*-polarized VNIR spectrum with the incident angle of the polarized light beam (see Figure 5a). A very similar observation was reported for LB films of OTiPc: the VNIR spectrum of an as-deposited LB film is almost identical with that in Figure 2a and a single XRD peak appears at $2\theta = 6.7^\circ$ ($d = 1.32$ nm).¹⁰ The peak at $2\theta = 6.85^\circ$ or 6.7° cannot be attributed to any XRD signal reported for solid OTiPc. It is therefore reasonable to deduce that an isotropic phase is grown under these conditions, keeping short-range molecular organization and preferential molecular alignment. Alternatively, a-S would be assignable as a disordered amorphous film containing domains of an unknown crystal phase. If this were the case, grains of the unknown crystal phase would have to be formed in a dominantly grown disordered amorphous phase under putting a particular lattice face in order. This is very unlikely to occur. As shown in Figure 3a, SEM observations of a-S indicate smooth and homogeneous features, suggesting that the contamination of different phases should be very minor if any.

A further support for the assignment of a-S was obtained from the phase change induced by CH₂Cl₂ vapor treatment.^{3,21,23,24} Upon exposure of a-S to saturated vapor of CH₂Cl₂ at room temperature for >12 h, the VNIR spectrum was changed to a much broader one essentially identical with that reported for α -OTiPc crystal (Figure 2a),^{8,20,21,25} and an intense XRD peak

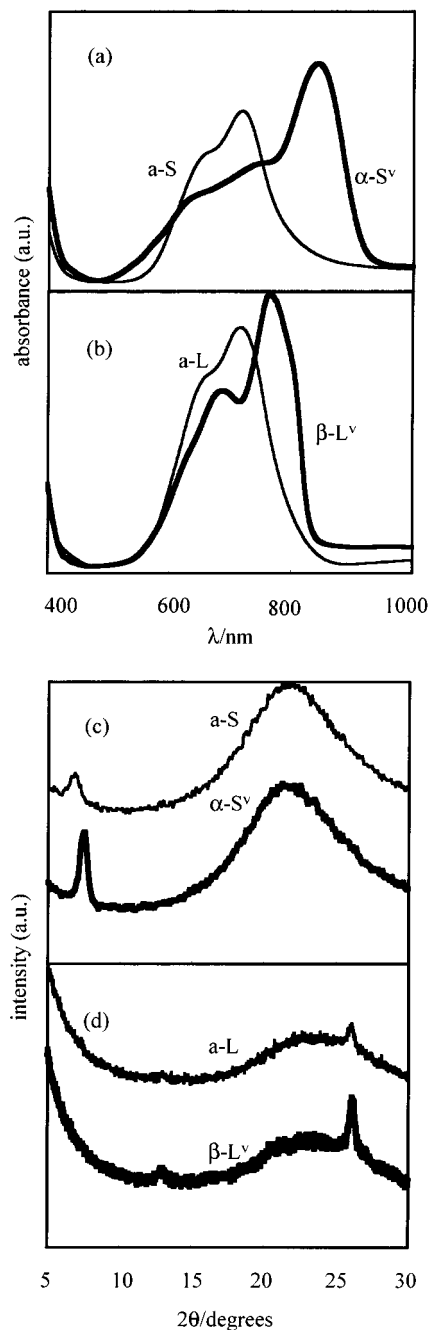


Figure 2. (Top) VNIR absorption spectra (a) for a-S and α -S^v (bold line) on glass and (b) for a-L and β -L^v (bold line) on Au/glass. (Bottom) XRD patterns (c) of a-S and α -S^v (bold line) on glass and (d) of a-L and β -L^v (bold line) on Au/glass; film thickness ≈ 150 nm.

appeared at $2\theta = 7.5^\circ$ ($d = 1.18$ nm) due to the diffraction from the (010) face of α crystal (Figure 2c).^{6,8,21} It can therefore be deduced that this vapor-

(23) Saito, T.; Sisk, W.; Kobayashi, T.; Suzuki, S.; Iwayanagi, T. *J. Phys. Chem.* **1993**, *97*, 8026.

(24) (a) Takano, S.; Mimura, Y.; Matsui, N.; Utsugi, K.; Gotoh, T.; Tani, C.; Tateishi, K.; Ohde, N. *J. Imaging Technol.* **1990**, *17*, 46.

(25) Mizuguchi, J.; Rihs, G.; Karfunkel, H. *J. Phys. Chem.* **1995**, *99*, 16217.

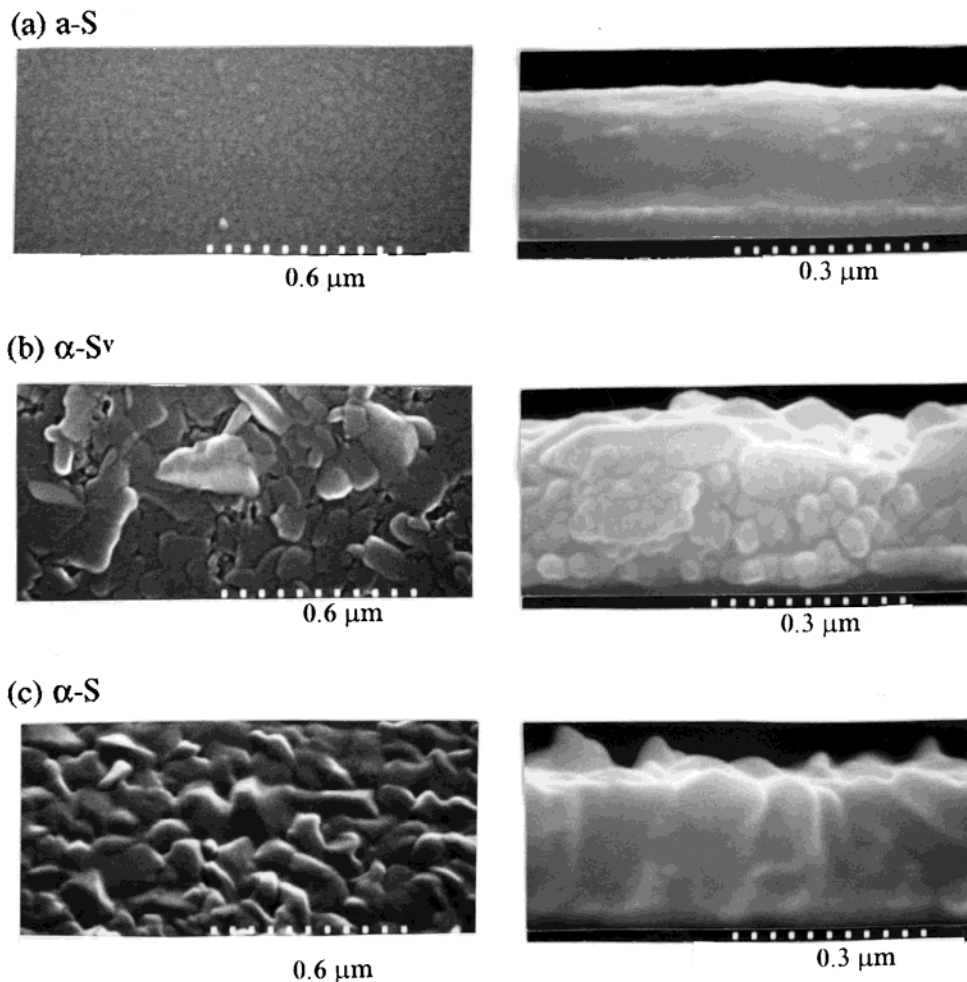


Figure 3. SEM photographs for (left) surface and (right) sectional views of (a) a-S on glass, (b) α -S^v on glass, and (c) α -S on Pt/glass; film thickness \approx 150 nm.

treated film dominantly consists of the α phase keeping the (010) lattice face parallel to the substrate surface (Figure 1a). This film is abbreviated as α -S^v for discrimination from the directly fabricated α -S films (vide infra). It is therefore reasonable to assume that relative molecular orientations in a-S are similar to those of α -S^v. In this regard, it should be noted that the vapor treatment of amorphous films obtained by deposition at $> 0.1 \text{ nm s}^{-1}$ gave disordered α -crystal films in which crystalline particles are randomly oriented.²¹ The vapor treatment does not align random molecular orientations in order but arranges orientational fluctuations to cause such minor displacements as a decrease from 1.29 to 1.18 nm in the repeated-layer distance.

The deposition onto Au and Ag/glass gave a different type of amorphous-like film denoted as a-L. This film shows a VNIR spectrum characteristic of amorphous OTiPc but no particular XRD signal except for a very weak peak at $2\theta = 26.2^\circ$ and the broad halo from the substrate. Upon treatment of a-L with CH_2Cl_2 vapor, the amorphous-like VNIR spectrum was changed to that characteristic of β -OTiPc ($\lambda_{\text{max}} = 780, 680 \text{ (sh) nm}$)^{8,20} and an intense XRD peak appeared at $2\theta = 26.2^\circ$ (Figure 2b,d). Since this XRD signal is characteristic of the (001) lattice plane of the β crystal,^{6,8,21} the vapor-treated film can be identified as a highly ordered film of the β phase keeping the (001) lattice face parallel to the substrate surface (Figure 1c). This film is denoted

as β -L^v. As discussed for a-S, therefore, it can be deduced that a-L should have similar lying orientations of OTiPc molecules, though the very weak XRD peak at $2\theta = 26.2^\circ$ indicates a very minor mixing of β -L domains. These findings strongly suggest that a-S and a-L have different molecular orientations though orientational fluctuations should more or less occur unlike the rigid arrangements in the crystal phases.

Deposition on Various Substrates Heated at 150 °C. The α -S^v and β -L^v films obtained by CH_2Cl_2 -vapor treatment of a-S and a-L are not morphologically uniform, consisting of various sizes of crystalline particles with substantial boundaries, as typically shown in Figure 3b for α -S^v. The CH_2Cl_2 -vapor treatment of a-S caused the growth of large crystallites, particularly in the surface region, accompanied by the substantial formation of grain boundaries due to volume shrinkages. When the substrate temperature was kept at $\geq 150^\circ\text{C}$, on the other hand, sufficiently good quality of ordered crystalline films were grown in thicknesses ranging from 50 to 500 nm, but the decrease of substrate temperature at $< 140^\circ\text{C}$ led to increasing losses of the crystallinity.

The deposition onto air-exposed Cu, Al, and Ti/glass as well as onto ITO-coated glass and neat glass heated at 150°C commonly gave α -S independently of the back pressures, whereas β -L was formed on Au and Ag/glass. In the case of Pt/glass, the deposition results were found

to depend on the back pressures. While α -S was grown under 1×10^{-3} – 4×10^{-4} Pa, the deposition under higher vacuum (2.7×10^{-5} Pa) gave a different film, α -L. In the above experiments, the vacuum of the chamber was broken prior to the OTiPc deposition following the metal coating on glass. For comparison, in situ OTiPc deposition was carried out without breaking the vacuum after the metal coating. Interestingly, β -L was formed on Cu/glass unexposed to air in contrast to the growth of α -S on air-exposed Cu/glass, whereas the deposition results in the other cases were independent of whether the substrates had been exposed to air. The surfaces of Al and Ti on glass should be oxidized upon exposure to air and even under 2.7×10^{-5} Pa during the deposition procedures,²⁶ whereas the surface oxidation of Cu occurs upon air exposure but not under the vacuum.

The morphological features of the crystalline films were analyzed by SEM. A typical example is shown in Figure 3c for α -S, revealing that the morphological features are considerably uniform with no indication of boundaries in sharp contrast to Figure 3b for α -S^v. The sectional view shows that single-crystal-like domains are grown along the full thickness (~ 150 nm) and closely adhere to each other to form a continuous monolithic phase. The film surface is densely packed with islands whose sizes are 100–150 nm. SEM observations of β -L again indicated smooth morphological features with grain sizes of 150–400 nm, but α -L showed the growth of various sizes of grains to give a relatively uneven sectional view though its morphology is much better than that of α -S^v (data not shown for β -L and α -L).

The assignment of α -S was performed by the exclusive appearance of an intense XRD peak at $2\theta = 7.5^\circ$ (Figure 4a) and by the VNIR absorption spectra characteristic of α -crystal (see Figure 5b). Similarly, β -L was identified on the basis of the appearance of an intense XRD signal at $2\theta = 26.2^\circ$ (Figure 4b) and the characteristic VNIR spectrum (see Figure 5d). On the other hand, α -L shows a very broad VNIR spectrum (see Figure 5c) which is α -crystal-like but significantly different from those reported for solid-state OTiPc.^{3,11,20–23,25,27–29} In XRD of this film (Figure 4c), two major peaks appear at $2\theta = 25.3^\circ$ and 28.6° which are due to the diffractions from the (-202) and (-212) faces of α -OTiPc, respectively.^{6,8} Therefore, α -L can be assigned as a film that mainly consists of the α phase keeping the ab plane of the unit cell parallel to the substrate surface (Figure 1b). Since another XRD peak at $2\theta = 26.2^\circ$ seems to be due to the (001) face of β -crystal, β -L might be mixed in the major α -L phase. However, little absorption of β -L was observed in the VNIR spectrum of α -L though the absorbance of β -L at 780 nm is considerably high (see Figure 5c,d). The contamination of β -L in the α -L film should be very minor, if any. Since the signal at $2\theta = 26.2^\circ$ is very intense compared with the others, it can appear in a significant intensity even with minor contamination of β -L.

The IR spectra of the crystalline films provided further insights into the molecular orientations. Figure 6 shows IR spectra taken by the reflection-absorption

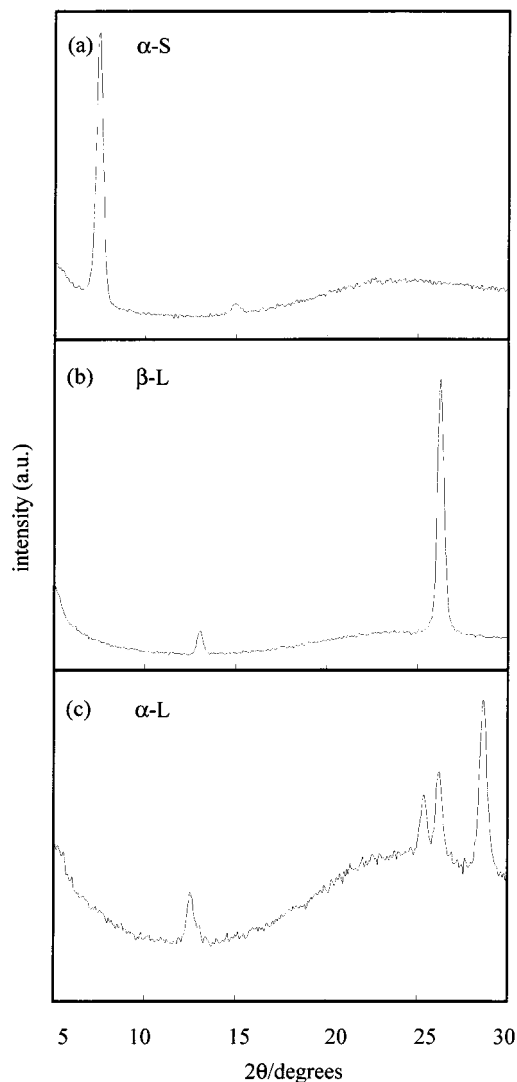


Figure 4. XRD patterns for (a) α -S on Pt/glass, (b) β -L on Au/glass, and (c) α -L on Pt/glass; film thickness ≈ 150 nm.

spectroscopic (RAS) method using p -polarized light. The incident angle was set at 80° so that the vibrational dipole components vertical to the substrate surface can be selectively picked up. The absorptions at 1120 and 1073 cm^{-1} for in-plane C–H deformation and at 960 – 973 cm^{-1} for out-of-plane Ti–O stretching vibration^{30,31} were used for the assignment of molecular orientations. As shown in Table 2, relative intensities ($I(\text{C–H})/I(\text{Ti–O})$) of the in-plane C–H deformation bands compared with the Ti–O stretching vibration band decrease in the order α -S $>$ α -L \gg β -L. In particular, the absorptions at 1000 – 1400 cm^{-1} for β -L are negligibly weak compared with the Ti–O stretching band, clearly demonstrating that OTiPc molecules are aligned with orientations almost parallel to the substrate surface (Figure 1c). This is in good agreement with the conclusion obtained from the XRD study. In the cases of α -S and

(26) (a) Nevin W. A.; Chamberlain, G. A. *IEEE Trans. Electron Devices* **1993**, *40*, 75. (b) Folkers, J. P.; Gorman, C. B.; Laibinis, P. E.; Buchhol, S.; Whitesides, G. M. *Langmuir* **1995**, *11*, 813.

(27) Hayashi, T.; Maruno, T.; Yamashita, A.; Fölsch, S.; Kambara, H.; Konami, H.; Hatano, M. *Jpn. J. Appl. Phys.* **1995**, *34*, 3884.

(28) Kofta, T. J.; Danziger, J.; Lee, P.; Pankow, J.; Nebesny, K. W.; Armstrong, N. R. *J. Phys. Chem.* **1987**, *91*, 5646.

(29) Ghosez, Ph. R.; Gastonguey, L.; Veilleux, G.; Den, G.; Dodelet, J. P. *Chem. Mater.* **1993**, *5*, 1581.

(30) Arco, R.; Thedchanamoorthy, A. *Chem. Mater.* **1995**, *7*, 69.

(31) Lever, A. B. P. *Adv. Inorg. Chem. Radiochem.* **1965**, *7*, 27.

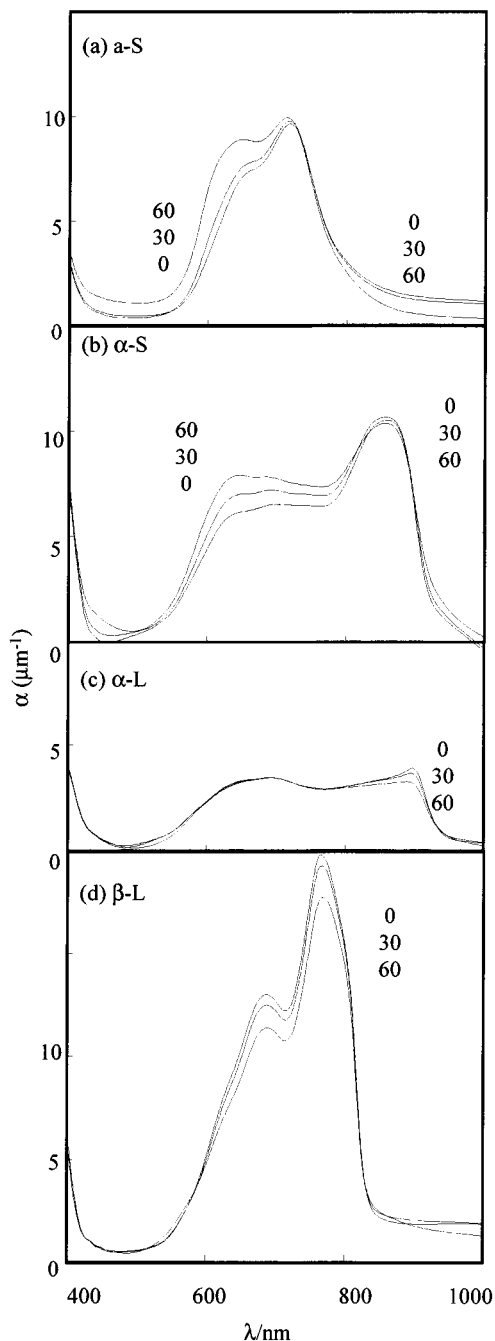


Figure 5. *p*-Polarized VNIR transmission-absorption spectra taken at various incident angles ($\theta = 0^\circ$, 30° , and 60°) for (a) α -S on Pt/glass, (b) α -S on Pt/glass, (c) α -L on Pt/glass, and (d) β -L on Au/glass; the numerals indicated denote the incident angles with respect to normal to the film surface. The unit in ordinate (α in μm^{-1}) is the absorbance corrected for unit film thickness ($1 \mu\text{m}$).

α -L, the in-plane vibration bands significantly appear unlike β -L, but the $I(\text{C-H})/I(\text{Ti-O})$ values for α -S are twice as high as those for α -L. This is again in accord with the assignments deduced from the XRD analysis that OTiPc molecules are aligned with an "obliquely standing" orientation in α -S but with a "lifted-lying" one in α -L (Figure 1a,b). According to the reported crystal structure of α -OTiPc,⁶ the pseudoplanar macrocycle makes an angle of $\sim 62^\circ$ with the (010) face (the *ac* plane) but an acute angle of $\sim 25^\circ$ with the *ab* plane; the *ac* and *ab* planes are parallel to the substrate surface in α -S and α -L, respectively.

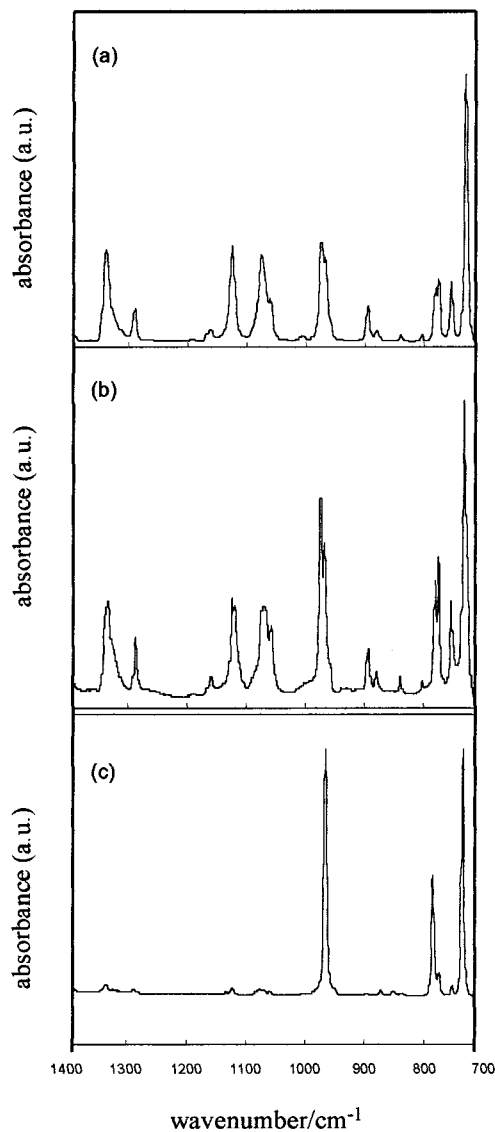


Figure 6. *p*-Polarized IR absorption spectra taken by the reflection-absorption method for (a) α -S on Pt/glass, (b) α -L on Pt/glass, and (c) β -L on Au/glass; film thickness $\approx 250 \text{ nm}$. The incident angle of the light beam with respect to normal to the film surface is 80° .

Table 2. Relative Intensities $I(\text{C-H})/I(\text{Ti-O})$ of IR Absorption Bands for In-Plane C-H Deformation vs Ti-O Stretching Vibration

methods	samples	$I(\text{C-H})/I(\text{Ti-O})^a$	
		1120 cm^{-1}	1073 cm^{-1}
RAS ^b	α -S	1.0	0.87
	α -L	0.52	0.45
	β -L	0.04	0.03
KBr ^c	α -crystal	2.2	2.1
	β -crystal	2.1	2.1

^a Relative intensities of the in-plane C-H deformation bands vs the out-of-plane Ti-O stretching vibration band at $\sim 970 \text{ cm}^{-1}$.

^b Measured for the deposited films by the reflection-absorption method using polarized light at an incident angle of 80° made by the light beam with normal to the film surface. ^c For crystalline powders dispersed in KBr disks.

The growth of the ordered solid films described above appears to be in line with the findings reported for MBD and MBE,^{18–20,27} highly ordered films are formed with "flat-lying" orientations on the Au (111), Cu (111), and Cu (100) faces¹⁸ for CuPc but with "standing" orienta-

tions on quartz for CuPc¹⁹ and on sapphire for OTiPc and OVPC.²⁰ The Ag, Au, and Cu substrates used in this work are polycrystalline films which have mainly the (111) face on their surfaces since they showed intense XRD peaks of the (111) face at $2\theta = 43.3^\circ$ (Ag), 38.2° (Au), and 38.1° (Cu). Therefore, layers might be grown with lying orientations on the Ag, Au, and Cu surfaces but with standing orientations on the surfaces of glass, ITO, and the surface-oxidized metals. In conventional vacuum deposition, the deposition rate should be prerequisite to preserving the molecular alignments. Vaporization of OTiPc at $\leq 0.05 \text{ nm s}^{-1}$ would generate individual molecules or small clusters to give initial ordered layers under interactions with the substrate surface,³² and accumulation of layers would give the meta-stable amorphous-like phases on the surfaces at $\sim 25^\circ\text{C}$ but the stable ordered α - or β -crystal phase on the surfaces heated at 150°C . However, it is still unknown why the deposition on Pt/glass heated at 150°C gave α -S under $\leq 10^{-4}$ Pa but α -L (not β -L) under 2.7×10^{-5} Pa.

Polarized VNIR Absorption Spectra. Figure 5 shows p -polarized VNIR absorption spectra taken by changing the incident angle (θ) made by the light beam normal to the film surface. Since the electric-field vector of p -polarized light oscillates in the plane normal to the film surface depending on θ , incident-angle dependences of the spectra provide significant information relevant to the electronic transitions of the films associated with the molecular orientations. In the cases of α -S and α -L, the increase of θ from 0° to 60° leads to similar changes, i.e., considerable increases of absorbance in the wavelength region shorter than the longest absorption maximum but small decreases at longer wavelength. This behavior suggests that α -S has a standing molecular alignment similar to that of α -L, if the electronic transition dipole moments for the absorption band are mainly in the molecular plane. On the other hand, both the spectrum and θ dependence of α -L are significantly different from those of α -S, indicating the anisotropic nature of electronic transitions in α crystal. The spectrum of β -L shows significant decreases of absorbance with the increase of θ over the full bandwidth. This behavior is not due to an experimental artifact but is real, since this θ dependence was reproduced. The incident angle dependence for β -L appears to accord with the "parallel" molecular alignment, provided that this film has the major electronic transition dipole moments in the molecular plane (vide infra). In the case of α -L, on the other hand, little incident-angle dependence was observed (data not shown), probably as the consequences of substantial fluctuations in molecular orientation.

The θ dependences coupled with the spectra seem to deserve some comments on the basis of the exciton coupling model³³ in relation with the electronic transitions of the α - and β -crystal films, though electronic absorption spectra of solid MPCs have been already discussed in terms of exciton splitting based on intermolecular π - π interactions,^{20,34} charge-transfer transi-

tions in J aggregate-like domains,²³ and molecular distortions caused by crystal packing.²⁵ The broad VNIR absorption bands of the films might arise, in appearance, from both blue- and redshifts of the Q-band ($\lambda_{\text{max}} = 690 \text{ nm}$ in CH_2Cl_2)^{10,35} by exciton couplings as observed for epitaxially grown films of perfluorinated ZnPc and OVPC.³⁶ When exciton couplings are considered for the nearest-neighbor pairs found in the α and β phases (see Figure 1 and ref 6), redshifts can occur with the in-line arrangements in the both phases and also for the coplaner inclined pairs with angles of 12.5° and 13.7° in the α phase or with an angle of 45° in the β phase, whereas the coplaner inclined couplings with angles of 58° and 62.9° in the α phase and the nonplaner one in the β phase can cause blueshifts. These exciton couplings give different transition dipoles which have components (D_{\parallel} and D , respectively) parallel and perpendicular to the substrate surface. Consequently, integrated relative contributions of D_{\parallel} and D should be changed with the change of θ and should be different in the red- and blueshifted regions. We carried out preliminary MO calculations using the reported crystal data, which gave satisfactory results for β -L but only poor results for α -S;³⁷ either the anisotropic spectra of α -S and α -L or their θ dependences were not well reproduced. Further works are in progress to explore the electronic transitions of the α phase using an in-plane ordered α -S film.^{37b}

Fluorescence Spectra. While the fluorescence behavior of MPC solids has been believed to provide an important mechanistic clue for the photogeneration of charge carriers,³ only a few systematic studies on the fluorescence of MPC solids have been performed,³⁸⁻⁴¹ probably because of experimental difficulties due to low emission efficiencies as well as to the emission wavelength region (800–1000 nm) where conventional detectors have little or no sensitivity. We performed preliminary fluorescence studies for the ordered films using the silicon-diode array detector which has sufficient sensitivities up to 1050 nm. Figure 7 shows typical fluorescence spectra taken at 293 (25°C) and 77 K for α -S and β -L, respectively. The fluorescence spectra of α -S and α -L are essentially identical, showing the maximum at

(34) Stillman, M. J.; Nyokong, T. In *Phthalocyanines: Properties and Applications*; Leznoff, C. C., Lever, A. B. P., Eds.; VCH Publishers: New York, 1989; Vol. 1, pp 133–289.

(35) Harazono, T.; Takagishi, I. *Bull. Chem. Soc. Jpn.* **1993**, *66*, 1016.

(36) (a) Schlettwein, D.; Hesse, K.; Tada, H.; Mashiko, S.; Storm, U.; Binder, J. *Chem. Mater.* **2000**, *12*, 989. (b) Schlettwein, D.; Tada, H.; Mashiko, S. *Langmuir* **2000**, *16*, 2872.

(37) (a) The calculations were performed for the pairs of distorted molecules found in the α and β crystals⁶ using the ZINDO/S program (HyperChem package, Hypercube Inc.) while the spectrum for an isolated nondistorted (structure-optimized) molecule was nicely simulated by ab initio MO calculations (SPARTAN, ver. 3.0.0, 3-21G) and by semiempirical MO calculations (MNDO, MOPAC 93). Details including simulations of highly anisotropic VNIR spectra of an in-plane ordered α -S film will be separately reported in near future. (b) The deposited films reported here are certainly ordered in orientations with respect to the substrate surface but not guaranteed for in-plane ordering.

(38) (a) Popovic, Z. D. *Chem. Phys.* **1984**, *86*, 311. (b) Popovic, Z. D. *J. Chem. Phys.* **1983**, *78*, 1552. (c) Popovic, Z. D.; Menzel, E. R. *J. Chem. Phys.* **1979**, *71*, 5090.

(39) (a) Popovic, Z. D.; Khan, M. I.; Atherton, S. J.; Hor, A.-M.; Goodman, J. L. *J. Phys. Chem. B* **1998**, *102*, 657. (b) Popovic, Z. D.; Hor, A. M. *Mol. Cryst. Liq. Cryst.* **1993**, *228*, 75.

(40) Yamaguchi, S.; Sasaki, Y. *J. Phys. Chem. B* **1999**, *103*, 6836.

(41) Gulvinas, V.; Jakubenas, R.; Pakalnis, S.; Undzenas, A. *Adv. Mater. Opt. Electron.* **1996**, *6*, 412.

(32) Schlettwein, D.; Graaf, H.; Meyer, J.-P.; Oekermann, T.; Jaefers, N. J. *J. Phys. Chem. B* **1999**, *103*, 3078.

(33) Kasha, M.; Rawls, H. R.; El-Bayoumi, M. A. *Pure Appl. Chem.* **1965**, *11*, 371.

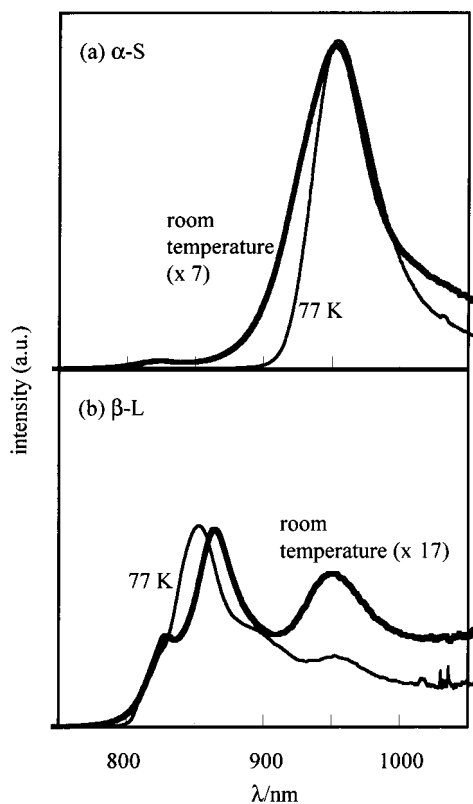


Figure 7. Normalized fluorescence spectra of (a) α -S on Pt/glass and (b) β -L on Au/glass; film thickness \approx 150 nm. The spectra at 298 K (bold line) are those magnified by a factor of 7 for α -S and by a factor of 17 for β -L for direct comparison with those at 77 K (faint line).

\sim 950 nm with relatively small separation from the absorption maximum (apparent Stokes shifts): \sim 1000 cm^{-1} for α -S and \sim 700 cm^{-1} for α -L. The fluorescence quantum yield for α -S was roughly estimated to be on the order of 10^{-3} at 293 K. The fluorescence of α -S also showed the maximum at \sim 950 nm largely separated from the absorption maximum though it is weaker than that of α -L. In the case of β -L, the fluorescence was again weaker than that of α -S and revealed different behavior; major maxima appear at 860 and 950 nm along with a minor one at 820 nm. At 77 K, the fluorescences of the solid films were considerably intensified with significant changes of the spectra as shown in Figure 7. In the case of β -L, in particular, an extra intensification around the 860 nm maximum accompanied by a 10 nm blueshift occurred, indicating that the 860 and 950 nm emissions arise from different sites in which the population of the 860 nm emission site would precede that of the other.

Both α -S and α -L have a dominant 950 nm-emission site close to the photoexcited singlet state, and this site is the major emissive state of α -S though it is separated with a relatively large energy gap from the initial excited state. On the other hand, the fluorescence of β -L occurs mainly from the 860 nm site and competitively from the 950 nm one. The 950 nm site appears to be commonly populated in the OTiPc solid films independently of the phases. Its population might occur by relaxation of or energy migration from the initial excited state in the α -phase films while energy migration from

the higher-energy 860 nm site to the 950 nm one should be involved in the case of β -L. The 950 nm site seems to be of interest related with carrier-generation mechanisms in the α and β phases, since the photoconductivity of a polymer-dispersed film of α -crystal particles was reported to be considerably higher than that of β -crystal particles.²³ Recently, it was reported that the photo-generation of charge carriers in the Y polymorph of OTiPc occurs from the emission sites.^{39,40} In this regard, it is of interest to note that the remarkable temperature dependences of the fluorescences imply the participation of an activated nonemissive pathway or pathways competing with the emission process or with the population of the emission sites from a common state. An attractive speculation is that a dominant activated pathway might be phonon-coupled charge separation associated with carrier generation. Further studies involving the static and time-resolved fluorescence behavior of the ordered OTiPc films are now underway in an attempt to obtain mechanistic molecular insights into the excited-state dynamic processes in the solid state of OTiPc.

Conclusions

The present investigation demonstrated that various ordered solid films of OTiPc are formed in 50–500 nm thickness by vacuum deposition onto such conventional substrates as metal/glass, ITO/glass, and neat glass at a rate of \sim 0.05 nm s^{-1} under 10^{-3} – 2.7×10^{-5} Pa. Deposition of OTiPc onto Pt/glass, ITO/glass, neat glass, and surface-oxidized Al, Ti, and Cu/glass at ambient temperature commonly gave α -S, whereas α -L was formed on Au and Ag/glass substrates. When the substrates were heated at 150 $^{\circ}\text{C}$, the α -S films were grown onto surface-oxidized Al, Ti, and Cu on glass, ITO/glass, and neat glass, but the β -L films onto Au, Ag, and unoxidized Cu/glass. In the case of Pt/glass heated at 150 $^{\circ}\text{C}$, the α -S films were grown under 10^{-3} – 10^{-4} Pa but the α -L films under 2.7×10^{-5} Pa. Morphological features of the ordered crystalline films observed by SEM indicated that single-crystal-like particles are grown in full thickness and densely packed with little boundary. These ordered films show unique features in the VNIR absorption spectra, which might provide significant insights into the anisotropic electronic structures of the OTiPc solid materials. The fluorescence spectra of the solid films were successfully measured to provide possible important clues for the excited-state behavior in the solid state. In preliminary experiments, we have confirmed that these ordered films of OTiPc are tough enough for sandwich-type diode cells to be constructed with ease and that the diode cells constructed show unique conductive behavior in the dark and under illumination depending on the molecular alignments of the films.

Acknowledgment. The authors are grateful to S. Matsumoto and H. Maki, at the Analysis Center of Dainippon Ink & Chemicals Co., for SEM and XRD measurements.

CM000766Y